NIH Public Access
Author Manuscript
Cell Microbiol. Author manuscript; available in PMC 2011 July 1.

Published in final edited form as:
Cell Microbiol. 2010 July ; 12(7): 919–929. doi:10.1111/j.1462-5822.2010.01440.x.

E. coli secreted protein F promotes EPEC invasion of intestinal epithelial cells via an SNX9-dependent mechanism

Andrew W Weflen[1], **Neal M Alto**[2], **V K Viswanathan**[3], and **Gail Hecht**[1]

[1] Department of Medicine, Section of Digestive Disease and Nutrition; University of Illinois at Chicago; Chicago, Il, 60612; USA.

[2] Department of Microbiology; The University of Texas Southwestern Medical Center at Dallas; Dallas, Tx, 75390; USA.

[3] Department of Veterinary Science and Microbiology; The University of Arizona; Tucson, AZ, 85721; USA.

SUMMARY

Enteropathogenic *E. coli* (EPEC) infection requires the injection of effector proteins into intestinal epithelial cells (IECs) via type three secretion. Type-three-secreted effectors can interfere with IEC signaling pathways via specific protein-protein interactions. For example, *E. coli* secreted protein F (EspF) binds sorting nexin 9 (SNX9), an endocytic regulator, resulting in tubulation of the plasma membrane. Our aim was to determine the mechanism of EspF/SNX9-induced membrane tubulation. Point mutation of the SNX9 lipid binding domains or truncation of the EspF SNX9 binding domains significantly inhibited tubulation, as did inhibition of clathrin coated pit (CCP) assembly. Although characterized as non-invasive, EPEC are known to invade IECs *in vitro* and *in vivo*. Indeed, we found significant invasion of Caco-2 cells by EPEC, which, like tubulation, was blocked by pharmacological inhibition of CCPs. Interestingly, however, inhibition of dynamin activity did not prevent tubulation or EPEC invasion, which is in contrast to *Salmonella* invasion, which requires dynamin activity. Our data also indicate that EPEC invasion is dependent on EspF and its interaction with SNX9. Together, these findings suggest that EspF promotes EPEC invasion of IECs by harnessing the membrane-deforming activity of SNX9.

INTRODUCTION

Many pathogenic bacteria of the gastrointestinal tract share a common infection strategy in which an array of highly evolved virulence factors are secreted directly into the cytosol of intestinal epithelial cells via a type three secretion system (T3SS) in order to disrupt host cell function and promote pathogenesis (Galan *et al.*, 2006; Moraes *et al.*, 2008). Detailed studies have revealed that these type 3 secreted effectors (T3SEs) have evolved to precisely target specific host pathways and control their activity to the benefit of the pathogen (Alto *et al.*, 2006; Stavrinides *et al.*, 2008). Enteropathogenic *E. coli* (EPEC) is a model organism in this respect, as it injects an array of T3SEs into epithelial cells of the small intestine, leading to dramatic alterations in cytoskeletal organization, ion transport, barrier function, regulation of cell death, and inflammatory signaling cascades (Kenny *et al.*, 1997; Crane *et al.*, 1999; McNamara *et al.*, 2001; Savkovic *et al.*, 2001; Matsuzawa *et al.*, 2004; Viswanathan *et al.*, 2004; Hodges *et al.*, 2008). Many of the EPEC T3SEs have been found to engage with specific host factors to affect such alterations (Gruenheid *et al.*, 2001; Viswanathan *et al.*,

Contact: Gail Hecht; gahecht@uic.edu; phone: 312-996-6651; fax: 312-996-5103; 840 S Wood St., Room 718E CSB (M/C 716), Chicago, Il 60612.

NIH-PA Author Manuscript
NIH-PA Author Manuscript
NIH-PA Author Manuscript

NIH-PA Author Manuscript

NIH-PA Author Manuscript

NIH-PA Author Manuscript

2004; Alto *et al.*, 2006). For example, recent studies by our lab and others have shown that the EPEC T3SE EspF participates in highly specific molecular interactions with the host protein sorting nexin 9 (SNX9), yet the significance of this interaction within the greater context of EPEC infection is unknown (Alto *et al.*, 2007; Marchès *et al.*, 2006).

EspF is one of the most studied among the EPEC T3SEs, with reported roles in antiphagocytosis, sodium transport inhibition, apoptosis, tight junction breakdown, intermediate filament degradation, and aquaporin redistribution (McNamara *et al.*, 2001; Viswanathan *et al.*, 2004; Nagai *et al.*, 2005; Quitard *et al.*, 2006; Guttman *et al.*, 2007; Hodges *et al.*, 2008). EspF contains three proline-rich repeats (PRRs) of approximately 45 residues each, which constitute the carboxy-terminal two-thirds of the protein and contain putative protein-protein interaction sites (Crane *et al.*, 2001; Marchès *et al.*, 2006; Alto *et al.*, 2007). Indeed, the SH3 binding sites within each of these PRRs interact exclusively with the SH3 domain of SNX9 (Alto *et al.*, 2007). The specificity of this interaction and the fact that it is conserved among the related pathogens EHEC and *Citrobacter rodentium* are indicative of a role for EspF/SNX9 binding in EPEC pathogenesis, yet no such role has been described.

SNX9 is a member of the sorting nexin family of mammalian proteins, which are involved in the regulation of vesicle trafficking and endocytosis. Sorting nexins are defined by the presence of a phox homology (PX) domain, which restricts these proteins to discreet subcellular compartments depending on its phospholipid specificity (Worby *et al.*, 2002; Lundmark *et al.*, 2009). SNX9, for instance, targets plasma membrane domains enriched in bis- and trisphosphorylated phosphatidylinositol molecules found at sites of clathrin-coated pit (CCP) formation (Lundmark *et al.*, 2003; Yarar *et al.*, 2008). This targeting specificity allows regulated recruitment of SNX9 and its binding partners to CCPs during clathrin-mediated endocytosis (CME) (Soulet *et al.*, 2005). Such partners include dynamin and N-WASP, which bind the amino-terminal SH3 domain of SNX9 and are thus recruited to CCPs during CME (Shin *et al.*, 2008). SNX9 also binds the clathrin adapter AP-2 along with clathrin itself via a low complexity region, which further enhances its localization to CCPs (Lundmark *et al.*, 2002). At the SNX9 c-terminus is a bin-amphiphysin-RVS (BAR) domain, another membrane interaction motif, which can sense membrane curvature and induce membrane tubulation (Pylypenko *et al.*, 2007; Shin *et al.*, 2008). This particular combination of protein and membrane interaction domains enables SNX9 to regulate several classes of endocytosis, including CME, by coupling membrane and actin remodeling to the spatial and temporal targeting and activation of endocytic accessory factors (Lundmark *et al.*, 2003; Yarar *et al.*, 2007; Lundmark *et al.*, 2009). Interestingly, EspF accumulates at CCPs with kinetics similar to SNX9 and in a manner dependent upon SNX9 interaction, although a link between CCP recruitment of EspF and EPEC pathogenesis has been elusive (Soulet *et al.*, 2005; Alto *et al.*, 2007). Furthermore, EspF/SNX9 interaction stimulates the formation of elongated, plasma membrane-derived tubular vesicles in both transfection and EPEC infection models (Alto *et al.*, 2007), suggesting that EspF can influence the regulation of CME by SNX9. Despite the connection between EspF, SNX9 and CME, the mechanism of tubule formation is not known, nor is it clear how activation of SNX9 by EspF relates to EPEC pathogenesis.

The aim of this study was to define the mechanism of EspF/SNX9-induced membrane tubulation and to establish a role for EspF/SNX9 interaction in EPEC pathogenesis. This interaction has been reported to be dispensable for intestinal barrier disruption and NHE3 downregulation, two phenotypes attributed to EspF and central to EPEC pathogenesis (Alto *et al.*, 2007; Hodges *et al.*, 2008). We report herein that EspF/SNX9-dependent membrane tubulation is sensitive to inhibitors of CCP assembly and requires functional lipid-binding domains of SNX9 as well as at least two SNX9 binding sites within EspF. Furthermore, we

NIH-PA Author Manuscript

NIH-PA Author Manuscript

NIH-PA Author Manuscript

found that EspF/SNX9 interaction enhances invasion of intestinal epithelial cells by EPEC and that invasion is also sensitive to inhibitors of CCP assembly. Although EPEC has been characterized as an extracellular pathogen, many reports clearly indicate the existence of intracellular EPEC in cell culture, animal models and human infection (Staley *et al.,* 1969; Tzipori *et al.,* 1985; Andrade *et al.,* 1989; Donnenberg *et al.,* 1989; Francis *et al.,* 1991; Scaletsky *et al.,* 1996; Jepson *et al.,* 2003; Bulgin *et al.,* 2009). Importantly, EspF has evolved a high degree of specificity for SNX9 and this interaction appears to be required exclusively for EPEC invasion, suggesting that invasion may be a bona-fide pathogenic phenotype of EPEC.

RESULTS

PX and BAR domains are required for EspF-induced membrane tubulation

EspF/SNX9 interaction induces the formation of irregular, plasma membrane-derived tubular vesicles that are sensitive to deletion of the SNX9 BAR domain (Alto *et al.,* 2007), however, such truncations have been suggested to exhibit altered protein folding and solubility (Yarar *et al.,* 2008; Lundmark *et al.,* 2009). To determine the importance of the PX and BAR domains in EspF/SNX9-induced tubular vesicles, we utilized a more discreet approach, in which membrane tubulation was assessed in HeLa cells co-transfected with EGFP-EspF and either mCherry-tagged wild-type SNX9 (mCherry-SNX9^{WT}) or SNX9 constructs encoding point mutations in the PX (mCherry-SNX9^{RYK}), BAR (mCherry-SNX9^{mutBAR2}), or both domains (mCherry-SNX9$^{RYK/mutBAR2}$). These point mutations have been shown to suppress PX and BAR activity without affecting protein solubility (Yarar *et al.,* 2008). Cells expressing EspF and wild-type SNX9 showed extensive membrane tubulation (Fig. 1A), as reported previously (Alto *et al.,* 2007). In contrast, co-transfection of EGFP-EspF with either mCherry-SNX9^{RYK}, mCherry-SNX9^{mutBAR2} or mCherry-SNX9$^{RYK/mutBAR2}$, did not induce tubule formation. Instead, EspF and SNX9 were found to co-localize in a punctate pattern. Interestingly, when the number of puncta per cell were quantified, we found that cells expressing mCherry-SNX9^{mutBAR2} contained significantly more puncta than those expressing mCherry-SNX9^{RYK}, while cells expressing mCherry-SNX9$^{RYK/mutBAR2}$ contained an intermediate level of punctate structures (Fig. 1E). These results indicate that EspF-induced tubulation requires fully functional PX and BAR domains.

EspF requires at least one PRR to induce membrane tubulation

Dynamin activity has been suggested to counteract SNX9-dependent membrane tubulation by inducing the budding of membrane vesicles, thus limiting the extent of tubule elongation (Shin *et al.,* 2008). In fact, expression of the PX-BAR domains of SNX9 is sufficient to induce extensive tubule formation, suggesting that uncoupling of dynamin activation from SNX9 membrane remodeling promotes tubulation (Pylypenko *et al.,* 2007). As EspF and dynamin both interact with the SH3 domain of SNX9, we postulated that EspF induces SNX9-mediated tubulation by excluding dynamin interaction, thus preventing the budding of membrane vesicles. If so, then expression of an EspF construct containing a single SNX9 binding site would be predicted to be sufficient to induce membrane tubulation. In order to test this prediction, we assessed membrane tubulation in HeLa cells transfected with mCherry-SNX9 and either EGFP alone, or EGFP fused to EspF-derived truncation constructs containing one, two, or three proline-rich repeats or a 15aa peptide corresponding to the SNX9-binding site (figure 2A). Expression of the SNX9 binding site alone (EspF$^{117-131}$) or an EspF construct truncated after the first PRR (EspF$^{1-119}$) was not sufficient to induce tubulation. Addition of the second PRR (EspF$^{1-166}$) and the third PRR (EspF^{WT}) significantly increased tubule formation (Fig. 2B, 2C). These results suggest that

NIH-PA Author Manuscript

NIH-PA Author Manuscript

NIH-PA Author Manuscript

dynamin exclusion alone is in fact not sufficient to induce tubulation, and that at least two SNX9 binding sites within EspF are required.

Membrane tubulation is blocked by inhibitors of CME

Examination of EspF-induced membrane tubules by transmission electron microscopy revealed that they are plasma membrane-derived (Alto *et al.,* 2007), yet it is unclear if they arise via a known endocytic pathway. Additionally, EspF has been shown to transiently associate with clathrin-coated pits (CCP), the timing of which is dependent upon EspF/SNX9 interaction, suggesting a clathrin-based mechanism for SNX9-dependent membrane tubulation (Alto *et al.,* 2007). We therefore assessed the effect of small molecule endocytic inhibitors on the formation of membrane tubules in cells co-expressing EGFP-EspF and mCherry-SNX9 (Fig. 3). Interestingly, the CME inhibitors chlorpromazine and monodansyl cadaverine both blocked the formation of membrane tubules, however treatment with the dynamin GTPase inhibitor dynasore and cholesterol extraction by methyl-β-cyclodextrin had no effect, suggesting that EspF stimulation of SNX9-mediated membrane tubulation requires CCP assembly, but not dynamin activity or lipid rafts.

EspF/SNX9 interaction enhances EPEC invasion of Caco-2 cells

Despite indications that EspF intersects with CME via SNX9 binding ((Alto *et al.,* 2007), this study), EspF/SNX9 interaction is dispensable for EspF-dependent affects on host cell processes involving endocytosis, such as NHE3 inhibition (Hodges *et al.,* 2008), and antiphagocytosis (data not shown). In addition, SNX9 interaction is dispensable for EspF-dependent tight junction disruption (Alto *et al.,* 2007). We therefore investigated the role of EspF/SNX9 interaction in another endocytosis-related EPEC phenotype, invasion of intestinal epithelial cells.

EPEC invasion was assessed by gentamicin protection assays of confluent Caco-2 monolayers infected with a range of MOIs from 0.3-300. As expected, increasing the MOI resulted in a greater number of total cell-associated bacteria as well as intracellular bacteria (Fig. 4A). Interestingly, however, at higher MOIs the proportion of total cell-associated bacteria that were intracellular decreased (Fig. 4B), suggesting that either EPEC are more efficient at invading Caco-2 cells at lower bacterial density, or that the cells become saturated with bacteria, limiting the rate of invasion at high MOI. Similar patterns have been observed with other bacterial species, and, indeed, we found the same relationship between MOI and invasion rate with *Salmonella* and *Shigella* (data not shown). To confirm the ability of EPEC to invade fully-differentiated intestinal epithelial cells, Caco-2 cells were grown on permeable supports for greater than 14 days and infected with WT EPEC. The cells were then fixed and processed for transmission electron microscopy. Intimately attached bacteria were present as defined by the characteristic membrane cup formation and electron-dense cytoskeletal material directly adjacent to bacteria (Fig. 4C, arrowheads). In addition, as indicated by arrows in Figure 4C, intracellular bacteria were clearly visible, confirming our gentamicin protection assay results and indicating that EPEC invades polarized intestinal epithelial cells.

In order to test the role of EspF in invasion of IECs, we performed gentamicin protection assays at an MOI of 0.3 in Caco-2 cells infected with WT EPEC and an *espF* knockout, Δ*espF*. Indeed, deletion of *espF* decreased EPEC invasion by approximately 50% as compared to WT (Fig. 4D). This defect was reversed by IPTG-inducible *espF* complementation in a dose-dependent manner, confirming the involvement of EspF in EPEC invasion of Caco-2 cells (Fig. 4D).

NIH-PA Author Manuscript

NIH-PA Author Manuscript

NIH-PA Author Manuscript

We next questioned the role of EspF/SNX9 interaction in EPEC invasion. We therefore tested the invasive capacity of Δ*espF* complemented with a plasmid encoding an *espF* gene containing point mutations in each of the three SNX9 binding motifs, which has been shown previously to be deficient for SNX9 interaction (Alto *et al.*, 2007). Strikingly, the EPEC strain expressing this mutant EspF exhibited the same invasion defect as the *espF* knockout strain (Fig. 4E), indicating that EspF involvement in EPEC invasion depends entirely upon its capacity to interact with SNX9.

EPEC invasion is blocked by inhibitors of CME

Our data show that both invasion and membrane tubulation are enhanced by EspF/SNX9 interaction, suggesting they occur by a similar endocytic mechanism. To test this, EPEC invasion was assessed in the presence of the same endocytic inhibitors that were found to block membrane tubulation. Both chlorpromazine and monodansyl cadaverine, inhibitors of clathrin-coated pit formation, decreased EPEC invasion significantly, indicating that EPEC indeed requires clathrin assembly for invasion (Fig. 5A). Additionally, cholesterol extraction via MBCD treatment had a significantly deleterious effect on EPEC invasion despite being ineffective at preventing membrane tubulation (Fig. 5A, Fig. 3). This discrepancy is likely due to the fact that MBCD is known to affect type three secretion efficiency (Allen-Vercoe *et al.*, 2006). This would be expected to inhibit EPEC invasion, however our tubulation experiments involved EspF transfection, thus eliminating effects related to type three secretion. Quite intriguing was the fact that dynasore did not block EPEC invasion, suggesting, as was observed with EspF-induced membrane tubulation, that EPEC invasion occurs via an SNX9- and clathrin-dependent mechanism that does not require dynamin activity. Furthermore, we found that invasion of *Salmonella* was sensitive to dynamin inhibition (Fig. 5B), confirming a previous report (Viega *et al.*, 2007) and highlighting the difference in invasion mechanism used by these two similar pathogens. Additionally, of the inhibitors found to block EPEC invasion, none protected against EPEC-induced TER loss (Fig. 5C). This supports the previous finding that EspF/SNX9 interaction is not required for EPEC-induced barrier disruption and indicates that EPEC invasion and membrane tubulation are independent from tight junction disruption.

EspF, clathrin and dynamin have all been reported to accumulate at sites of EPEC attachment (Unsworth *et al.*, 2006; Viega *et al.*, 2007). To confirm this in our model system, HeLa cells were transfected with either EGFP-EspF, YFP-clathrin light chain or EGFP-dynamin II and infected with wild-type EPEC. Indeed, all three proteins were enriched at sites directly adjacent to attached bacteria (Fig. 5D). This is consistent with the role of EspF and clathrin in EPEC invasion, however, as we found dynamin activity to be dispensable for invasion, its localization to attached EPEC is likely related to its reported role in pedestal formation (Unsworth *et al.*, 2006), which is independent of EPEC invasion (Jepson *et al.*, 2003).

SNX9 contributes to EPEC invasion of Caco-2 cells

In order to confirm the importance of SNX9 in EPEC invasion, we conducted gentamicin protection assays in Caco-2 cells after SNX9 knock-down. siRNA treatment significantly reduced SNX9 expression as determined by Western blot analysis (Fig. 6A). Interestingly, SNX9 knockdown decreased EPEC invasion (Fig. 6C) to a similar degree as did EspF deletion or expression of the SNX9 binding mutant (Fig. 4E). Despite the fact that EspF/SNX9 interaction is required for invasion, we found that SNX9 recruitment to EPEC microcolonies was independent of EspF (Fig. 6E), suggesting that recruitment alone is not sufficient to enhance invasion, but that activation of EPEC-associated SNX9 by EspF is required. Together, these data indicate that SNX9 indeed plays a role in EPEC invasion. To determine if SNX9 activity is a common mechanism for bacterial invasion, we also tested

NIH-PA Author Manuscript

NIH-PA Author Manuscript

NIH-PA Author Manuscript

Salmonella invasion of Caco-2 cells treated with siRNA. In stark contrast to our results with EPEC, *Salmonella* invasion was not affected by SNX9 knockdown (Fig. 6D), demonstrating that the role of SNX9 in EPEC invasion does not extend to all bacterial pathogens and may represent a novel pathway for bacterial entry into epithelial cells.

DISCUSSION

The three PRDs of EspF bind the SH3 domain of SNX9 with a high degree of specificity (Marchès *et al.*, 2006; Alto *et al.*, 2007). Although this interaction is specific for SNX9 but not other SH3 proteins and occurs during EPEC infection (Alto *et al.*, 2007), SNX9 interaction has not been attributed to any EspF-dependent phenotype to date (Marchès *et al.*, 2006; Alto *et al.*, 2007; Hodges *et al.*, 2008). In the present study, we show that EspF/SNX9 interaction promotes EPEC invasion of intestinal epithelial cells and membrane tubulation, both of which require CCP assembly but not dynamin activity. The similarities between tubulation and invasion point to a model in which EPEC invasion is enhanced by EspF-mediated activation of SNX9-dependent membrane remodeling. Based on data presented herein and in previous reports, we propose a model in which SNX9 promotes EPEC invasion via a multi-step process, requiring recruitment to the plasma membrane, oligomerization, membrane deformation and actin polymerization (Fig. 7). This process may be initiated by EPEC-induced alterations in the plasma membrane, such as formation of curved membrane surfaces (Fig. 4C, arrowheads), PIP accumulation (Sason *et al.*, 2009) and clustering of the tyrosine-phosphorylated membrane receptor Tir (Touze *et al.*, 2004). Similar membrane topography occurs at sites of tyrosine-phosphorylated receptor clustering just prior to CME (Conner *et al.*, 2003) and likely contributes to the recruitment of clathrin by EPEC (Fig. 5D, 7A). We predict SNX9 recruitment to be enhanced by these factors as well as by the presence of clathrin (Lundmark *et al.*, 2009), which would provide a mechanistic explanation for the lack of EspF involvement in SNX9 accumulation (Fig. 6E, 7B). The finding that EspF deletion inhibits EPEC invasion but not SNX9 recruitment suggests that recruitment alone is insufficient for SNX9-induced invasion, but that subsequent activation by EspF is required. EspF concentrations are likely to be greatest immediately adjacent to attached bacteria, positioning the effector to interact with bacterially-associated SNX9, thus leading to the displacement of dynamin (Fig. 7C). Dynamin recruitment by EPEC has been reported to promote pedestal formation (Unsworth *et al.*, 2006), providing an alternative explanation for its presence under EPEC microcolonies. However, pedestal formation is dispensable for invasion (Jepson *et al.*, 2003), which is consistent with our finding that dynamin inhibition does not block invasion (Fig. 5A). Unlike dynamin, EspF contains multiple SNX9 binding sites, potentially allowing interaction with up to three SNX9 molecules. This may have a cross-linking affect, promoting SNX9 oligomerization and, in turn, amplifying its activity resulting in spatially restricted deformation of the plasma membrane directly adjacent to bacteria, thus promoting invasion (Fig. 7D). In addition, EspF possesses three N-WASP binding sites (Alto *et al.*, 2007), which could allow EspF to couple SNX9-mediated membrane remodeling to N-WASP-dependent actin polymerization and enhance membrane engulfment of EPEC (Fig. 7D).

SNX9 requires both the PX and BAR domains for plasma membrane targeting and deformation (Pylypenko *et al.*, 2007; Yarar *et al.*, 2008; Lundmark *et al.*, 2009). Accordingly, we found that point mutation of either domain severely attenuated EspF-induced tubule formation. Furthermore, co-expression of the PX and BAR mutants and EspF led to co-localization at punctate locations within the cell in a pattern reminiscent of SNX9 recruitment to CCPs (Soulet *et al.*, 2005; Yarar *et al.*, 2008). Interestingly, Yarar et al found that the BAR mutant was recruited to CCPs less frequently than the PX mutant, which is the opposite of what we find in the context of EspF transfection (Fig. 1E). We speculate that this

NIH-PA Author Manuscript

NIH-PA Author Manuscript

NIH-PA Author Manuscript

may be due to the fact that EspF can potentially interact with multiple SNX9 molecules and thus promote SNX9 oligomerization. As the BAR mutation was predicted to affect the capacity of SNX9 to dimerize (Yarar *et al.*, 2008), EspF could compensate for this defect by bringing several SNX9 monomers together, increasing membrane targeting of the complex but not improving the membrane deforming capacity of this mutant BAR domain. Indeed, the finding that EspF requires two or three SNX9 binding sites to generate membrane tubules supports this interpretation.

Models of CME predict that SNX9 is involved in forming the neck of CCVs via the tubulating activity of the BAR domain immediately prior to dynamin-mediated vesicle fission (Lundmark *et al.*, 2009). If SNX9/dynamin interaction is prevented, either by binding of EspF or by deletion of the SH3 domain, dynamin cannot initiate vesicle budding, and extensive SNX9-induced tubulation occurs (Pylypenko *et al.*, 2007). This idea is supported by the finding that dynamin counteracts the formation of elongated tubules (Shin *et al.*, 2008). Interestingly, binding of the SH3 domain of SNX9 alone is necessary but not sufficient for tubulation, as our $EspF^{117-131}$ or $EspF^{1-119}$ constructs were deficient for tubule formation, suggesting that EspF requires multiple SNX9 binding sites for this activity. Taken together, these observations suggest that upon SNX9 recruitment to the plasma membrane, EspF binds to multiple SNX9 SH3 domains, thereby preventing SNX9/dynamin interaction and concomitant vesicle fission, and induces the formation of EspF/SNX9 oligomers, resulting in unrestricted membrane tubulation.

Precedent exists for pathogenically-significant, low-level invasion of bacteria previously thought to be strictly extracellular pathogens. For instance, uropathogenic *E. coli*, long believed to be non-invasive, was subsequently found to establish intracellular niches within bladder epithelial cells (Mulvey *et al.*, 1998). In the case of UPEC, invasion and intracellular survival allow the bacteria to establish a reservoir that is resistant to clearance, thus leading to persistence within the host and recurrent infections (Bower *et al.*, 2005). Similarly, *Helicobacter pylori*, another low-level invasive pathogen that was once thought to be solely extracellular, has since been found to utilize invasion as a way to establish chronic infection (Bjorkholm *et al.*, 2000). UPEC and *H. pylori* differ from classically invasive pathogens, such as *Shigella*, in that invasion is not absolutely required for pathogenesis, yet, under certain circumstances, these organisms exploit invasion to extend host colonization. Certainly, similarities exist between these two organisms and EPEC, in that they are not highly invasive, yet they have been observed intracellularly and are sometimes associated with persistent or recurrent infection (Scaletsky *et al.*, 1996; Abba *et al.*, 2009). Indeed, persistent EPEC infection may provide a clinical scenario in which invasion is relevant to disease, especially in view of the fact that atypical EPEC, which lack the 60kb *E. coli* adherence factor plasmid found in typical EPEC, are both more invasive and more often associated with persistent diarrhea (Scaletsky *et al.*, 1999; Asfet *et al.*, 2004; Hernandes *et al.*, 2008).

EXPERIMENTAL PROCEDURES

Cell culture and reagents

Caco-2 (ATCC HTB-37) and HeLa (ATCC CCL-2) cells were maintained following ATCC propagation and subculturing guidelines. Chlorpromazine (60μM), monodansyl cadaverine (400μM) and methyl-β-cyclodextrin (10mM) were from Sigma-Aldrich (St. Louis, MO). Dynasore (80μM) was synthesized by Dr. Henry E. Pelish and provided as a generous gift of Thomas Kirchhausen.

NIH-PA Author Manuscript

NIH-PA Author Manuscript

NIH-PA Author Manuscript

Antibodies and western blotting

For western blots, cells were rinsed twice in PBS and extracted in RIPA buffer (150mM NaCl, 100mM Tris-HCL (pH 7.4), 1% SDS, 0.1% Triton X-100, 1% Sigma protease inhibitor cocktail, 1mM PMSF, 1mM Na orthovanadate). Lysates were sonicated and centrifuged at 12,000×g for 20 minutes. Protein concentration of the supernatants was determined by the DC protein assay (Bio-Rad) and lysates were diluted 1:1 with 2x Laemmli sample buffer (Bio-Rad), boiled and loaded onto 12% SDS-PAGE gels. Proteins were transferred to nitrocellulose and probed with antibodies for SNX9 or actin where indicated. For immunoblotting, rabbit polyclonal anti-SNX9 antibodies (Soulet *et al.*, 2005) were diluted 1:1000, rabbit polyclonal anti-actin antibodies (Sigma-Aldrich) were diluted 1:5000 and HRP-conjugated goat anti-rabbit antibodies were used at a dilution of 1:5000.

Plasmids

pmCherry-SNX9, pmCherry-SNX9^{RYK}, pmCherry-SNX9^{mutBAR2}, and pmCherry-SNX9$^{RYK/mutBAR2}$ (Yarar *et al.*, 2008) were generous gifts of Sandra Schmid. EGFP-dynamin and YFP-clathrin light chain were generous gifts of Jerrold Turner. pEGFP-EspF was created as described previously (Alto *et al.*, 2007).

Transfections

HeLa cells were seeded onto glass coverslips at a density of $5x10^4$ cells/cm^2 and transfected with pmCherry-SNX9 and EGFP-EspF using Lipofectamine 2000 (Invitrogen) following the manufacturer's instructions. Sequences of SNX9 siRNA and scrambled oligonucleotides were described previously (Soulet *et al.*, 2005). RNA was introduced into Caco-2 cells using the Amaxa nucleofection kit (Lonza, Basel, Switzerland) following the manufacturer's instructions and SNX9 protein levels assessed at 1, 2, 3 and 4 days post-transfection by western blot.

Wide Field Epifluorescence Microscopy

After transfection and inhibitor treatment, HeLa cells were rinsed twice in PBS and fixed for 10 minutes at room temperature in 3.7% paraformaldehyde. Cells were then washed 5 times in PBS and mounted onto glass microscope slides using ProLong Gold Antifade Solution (Invitrogen, Carlsbad, Ca). Mounting solution was allowed to cure overnight at room temperature in the dark, and then specimens were examined using a Leica DM4000B epifluorescence microscope (Leica Microsystems, Wetzlar, Germany) equipped with a Retiga Exi CCD camera (Qimaging, Surrey, BC, Canada). Images were acquired and processed using SlideBook 4.2 software (Intelligent Imaging Innovations, Denver, Co).

Transmission Electron Microscopy

Caco-2 cells were grown on Transwell permeable supports (Corning) until fully differentiated (14-21 days) and infected with WT EPEC for 6 hours. Monolayers were then rinsed twice in warm PBS and fixed in 2.5% glutaraldehyde in 0.1M Na cacodylate buffer, pH 7.4, overnight at 4° C. Specimens were post-fixed in 1% osmium tetroxide in cacodylate buffer and dehydrated with a series of ethanol up to 100% absolute. Samples were then embedded in LX112 epoxy resin and microtome sections mounted on 200 mesh copper grids stained with 2% aqueous uranyl acetate and lead citrate. Grid sections were imaged using a JEM-1220 785 Erlangshen ES100W transmission electron microscope at 40kV to 120kV ACC voltage.

Gentamicin protection assays

To quantitate bacterial invasion, Caco-2 cells were seeded into duplicate 24-well plates at a density of 2.5×10^5 cells/well. Two days post-seeding, bacterial strains were inoculated into

NIH-PA Author Manuscript

NIH-PA Author Manuscript

NIH-PA Author Manuscript

Luria-Bertani broth containing selective antibiotics when appropriate and incubated overnight at 37°C with shaking. Three days post-seeding, bacterial overnight cultures were diluted into serum-free DMEM containing IPTG and grown to mid-log phase, corresponding to an OD of 0.4-0.6. Bacterial cultures were normalized to the same OD, and used to infect two plates of confluent Caco-2 monolayers in triplicate at the indicated MOI. Aliquots of bacterial cultures were diluted in PBS and spread on LB agar plates to determine CFU/mL of inoculum and additional wells of Caco-2 cells were trypsinized and cells/well determined by trypan blue staining to calculate MOI. Infected Caco-2 cells were incubated at 37°C in 5% CO_2 for 3 hours. To determine total cell-associated bacteria, one of the infected plates was removed from the incubator, rinsed in warm PBS to remove unattached bacteria, and incubated in 200uL of 1% Triton X-100 in PBS at 4°C for 10 minutes to liberate intracellular bacteria. The other plate was rinsed in warm PBS and incubated for 1 hour at 37°C in 5% CO_2 in the presence of 100ug/mL gentamicin (Sigma) in serum-free DMEM to kill extracellular bacteria. Cells were then rinsed in warm PBS, and treated with Triton X-100 as above. To enumerate intracellular or total cell-associated bacteria, each well was rinsed with cold PBS, which was then serial diluted and spread onto LB agar plates. Isolated colonies were then counted the following day after overnight incubation at 37°C in 5% CO_2.

Statistical analysis

All data are representative of at least three independent experiments. Results of gentamicin protection assays are reported as relative invasion. To determine relative invasion, rates of intracellular bacteria were represented by three calculations: total intracellular CFU/well, intracellular CFU/well as a percent of inoculum, and intracellular CFU/well as a percent of total cell-associated CFU/well. Wild-type EPEC invasion was normalized to a value of 1 for each calculation, and the average of the three normalized values expressed as relative invasion, thus providing a comprehensive evaluation of the invasion rate. For reference, in all experiments, a relative invasion of 1 corresponded to 10% of total cell-associated bacteria that were resistant to gentamicin killing. Asterisks indicate a p-value of <0.05 as determined by ANOVA.

Acknowledgments

We would like to thank Linda Juarez at the University of Illinois at Chicago Research Resources Center for assistance with TEM sample preparation and image acquisition. This work was supported by grants from the National Institutes of Health to G.H. (DK-50694 and DK-67887) and the Veterans Affairs Merit Review. N.M.A is supported by 1RO1AI083359-01.

REFERENCES

Abba K, Sinfield R, Hart CA, Garner P. Pathogens associated with persistent diarrhoea in children in low and middle income countries: a systematic review. BMC Infect Dis. 2009; 9

Allen-Vercoe E, Waddell B, Livingstone S, Deans J, DeVinney R. Enteropathogenic Escherichia coli Tir translocation and pedestal formation requires membrane cholesterol in the absence of bundle-forming pili. Cell Microbiol. 2006; 8:613–624. [PubMed: 16548887]

Alto NM, Shao F, Lazar CS, Brost RL, Chua G, Mattoo S, et al. Identification of a bacterial type III effector family with G protein mimicry functions. Cell. 2006; 124:133–145. [PubMed: 16413487]

Alto NM, Weflen AW, Rardin MJ, Yarar D, Lazar CS, Tonikian R, et al. The type III effector EspF coordinates membrane trafficking by the spatiotemporal activation of two eukaryotic signaling pathways. J Cell Biol. 2007; 178:1265–1278. [PubMed: 17893247]

Andrade JRC, Da Viega VF, De Santa Rosa MR, Suassuna I. An endoctyic process in HEp-2 cells induced by enteropathogenic Escherichia coli. J Med Microbiol. 1989; 28:49–57. [PubMed: 2643705]

NIH-PA Author Manuscript

NIH-PA Author Manuscript

NIH-PA Author Manuscript

Asfet JE, Bevanger L, Romundstad P, Bergh K. Association of atypical enteropathogenic Escherichia coli (EPEC) with prolonged diarrhoea. J Med Microbiol. 2004; 53:1137–1144. [PubMed: 15496393]

Bjorkholm B, Zhukhovitsky V, Lofman C, Hulten K, Enroth H, Block M, et al. Helicobacter pylori entry into human gastric epithelial cells: A potential determinant of virulence, persistence, and treatment failures. Helicobacter. 2000; 5:148–154. [PubMed: 10971679]

Bower JM, Eto DS, Mulvey MA. Covert operations of uropathogenic Escherichia coli within the urinary tract. Traffic. 2005; 6:18–31. [PubMed: 15569242]

Bulgin R, Arbeloa A, Goulding D, Dougan G, Crepin VF, Raymond B, Frankel G. The T3SS effector EspT defines a new category of invasive enteropathogenic *E. coli* (EPEC) which form intracellular actin pedestals. PLoS Pathog. 2009; 5:e1000683. [PubMed: 20011125]

Conner SD, Schmid SL. Regulated portals of entry into the cell. Nature. 2003; 422:37–44. [PubMed: 12621426]

Donnenberg MS, Donohue-Rolfe A, Keusch GT. Epithelial cell invasion: an overlooked property of enteropathogenic Escherichia coli (EPEC) associated with the EPEC adherence factor. J Infect Dis. 1989; 160:452–459. [PubMed: 2668429]

Francis CL, Jerse AE, Kaper JB, Falkow S. Characterization of interactions of enteropathogenic Escherichia coli O127:H6 with mammalian cells in vitro. J Infect Dis. 1991; 164:693–703. [PubMed: 1680136]

Galan JE, Wolf-Watz H. Protein delivery into eukaryotic cells by type III secretion machines. Nature. 2006; 444:567–573. [PubMed: 17136086]

Gruenheid S, DeVinney R, Bladt F, Goosney D, Gelkop S, Gish GD, et al. Enteropathogenic E. coli Tir binds Nck to initiate actin pedestal formation in host cells. Nat Cell Biol. 2001; 3:856–859. [PubMed: 11533668]

Guttman JA, Samji FN, Li Y, Deng W, Lin A, Finlay BB. Aquaporins contribute to diarrhoea caused by attaching and effacing bacterial pathogens. Cell Microbiol. 2007; 9:131–141. [PubMed: 16889624]

Hernandes RT, Sliva RM, Carneiro SM, Salvador FA, Fernandes MC, Padovan AC, et al. The localized adherence pattern of an atypical enteropathogenic Escherichia coli is is mediated by intimin omicron and unexpectedly promotes HeLa cell invasion. Cell Microbiol. 2008; 10:415–425. [PubMed: 17910741]

Hodges K, Alto NM, Ramaswamy K, Dudeja PK, Hecht G. The enteropathogenic Escherichia coli effector protein EspF decreases sodium hydrogen exchanger 3 activity. Cell Microbiol. 2008; 10:1735–1745. [PubMed: 18433466]

Jepson MA, Pellegrin S, Peto L, Banbury DN, Leard AD, Mellor H, Kenny B. Synergistic roles for the Map and Tir effector molecules in mediating uptake of enteropathogenic Escherichia coli (EPEC) into nonphagocytic cells. Cell Microbiol. 2003; 5:773–783. [PubMed: 14531893]

Lundmark R, Carlsson SR. The beta-appendages of the four adaptor-protein (AP) complexes: structure and binding properties, and identification of sorting nexin 9 as an accessory protein to AP-2. Biochem J. 2002; 362:597–607. [PubMed: 11879186]

Lundmark R, Carlsson SR. Sorting nexin 9 participates in clathrin-mediated endocytosis through interaction with the core components. J Biol Chem. 2003; 278:46772–46781. [PubMed: 12952949]

Lundmark R, Carlsson SR. SNX9 - a prelude to vesicle release. J Cell Sci. 2009; 122:5–11. [PubMed: 19092055]

Marchès O, Batchelor M, Shaw RK, Patel A, Cummings N, Nagai T, et al. EspF of enteropathogenic Escherichia coli binds sorting nexin 9. J Bacteriol. 2006; 188:3110–3115. [PubMed: 16585770]

McNamara BP, Koutsouris A, O'Connell CB, Nougayrede JP, Donnenberg MS, Hecht G. Translocated EspF protein from enteropathogenic Escherichia coli disrupts host intestinal barrier function. J Clin Invest. 2001; 107:621–629. [PubMed: 11238563]

Moraes TF, Spreter T, Strynadka NC. Piecing together the type III injectisome of bacterial pathogens. Curr Opin Struct Biol. 2008; 18:258–266. [PubMed: 18258424]

NIH-PA Author Manuscript

NIH-PA Author Manuscript

NIH-PA Author Manuscript

Mulvey MA, Lopez-Boado YS, Wilson CL, Roth R, Parks WC, Heuser J, Hultgren SJ. Induction and evasion of host defenses by type-1 piliated uropathogenic Escherichia coli. Science. 1998; 282:1494–1497. [PubMed: 9822381]

Nagai T, Abe A, Sasakawa C. Targeting of enteropathogenic Escherichia coli EspF to host mitochondria is essential for bacterial pathogenesis: critical role of the 16th leucine residue in EspF. J Biol Chem. 2005; 280:2998–3011. [PubMed: 15533930]

Pylypenko O, Lundmark R, Rasmuson E, Carlsson SR, Rak A. The PX-BAR membrane remodeling unit of sorting nexin 9. EMBO J. 2007; 26:4788–4800. [PubMed: 17948057]

Quitard S, Dean P, Maresca M, Kenny B. The enteropathogenic Escherichia coli EspF effector molecule inhibits PI-3 kinase-mediated uptake independently of mitochondrial targeting. Cell Microbiol. 2006; 8:972–981. [PubMed: 16681838]

Sason H, Milgrom M, Weiss AM, Melamed-Book N, Balla T, Grinstein S, et al. Enteropathogenic Escherichia coli subverts phosphatidylinositol 4,5-bisphosphate and phosphatidylinositol 3,4,5-trisphosphate upon epithelial cell infection. Mol Biol Cell. 2009; 20:544–555. [PubMed: 18987340]

Scaletsky IC, Pedroso MZ, Fagundes-Neto U. Attaching and effacing enteropathogenic Escherichia coli O18ab invades epithelial cells and causes persistent diarrhea. Infect Immun. 1996; 64:4876–4881. [PubMed: 8890257]

Scaletsky IC, Pedroso MZ, Oliva CA, Carvalho RL, Morais MB, Fagundes-Neto U. A localized adherence-like pattern as a second pattern of adherence of classic enteropathogenic Escherichia coli to Hep-2 cells that is associated with infantile diarrhea. Infect Immun. 1999; 67:3410–3415. [PubMed: 10377120]

Shin N, et al. SNX9 regulates tubular invagination of the plasma membrane through interaction with actin cytoskeleton and dynamin 2. J Cell Sci. 2008; 121:1252–1263. [PubMed: 18388313]

Soulet F, et al. SNX9 regulates dynamin assembly and is required for efficient clathrin-mediated endocytosis. Mol Biol Cell. 2005; 16:2058–2067. [PubMed: 15703209]

Staley TE, Jones EW, Corley LD. Attachment and penetration of Escherichia coli into intestinal epithelium of the ileum in newborn pigs. Am J Pathol. 1969; 56:371–392. [PubMed: 4898367]

Stavrinides J, McCann HC, Guttman DS. Host-pathogen interplay and the evolution of bacterial effectors. Cell Microbiol. 2008; 10:285–292. [PubMed: 18034865]

Touze T, Hayward RD, Eswaran J, Leong JM, Kornonakis V. Self-association of EPEC intimin mediated by the beta-barrel-containing anchor domain: a role in clustering of the Tir receptor. Mol Microbiol. 2004; 51:73–87. [PubMed: 14651612]

Tzipori S, Robins-Browne RM, Gonis G, Hayes J, Withers M, McCartney E. Enteropathogenic Escherichia coli enteritis: evaluation of the gnotobiotic piglet as a model of human infection. Gut. 1985; 26:570–578. [PubMed: 3924746]

Unsworth KE, Mazurkiewicz P, Senf F, Zettl M, McNiven M, Way M, Holden DW. Dynamin is required for F-actin assembly and pedestal formation by enteropathogenic *Escherichia coli* (EPEC). Cell Microbiol. 2006; 9:438–449. [PubMed: 16965516]

Viega E, Guttman JA, Bonazzi M, Boucrot E, Toledo-Arana A, Lin AE, et al. Invasive and adherent bacterial pathogens co-opt host clathrin for infection. Cell Host Microbe. 2007; 2:340–351. [PubMed: 18005755]

Viswanathan VK, Lukic S, Koutsouris A, Miao R, Muza MM, Hecht G. Cytokeratin 18 interacts with the enteropathogenic Escherichia coli secreted protein F (EspF) and is redistributed after infection. Cell Microbiol. 2004; 6:987–997. [PubMed: 15339273]

Worby CA, Dixon JE. Sorting out the cellular functions of sorting nexins. Nat Rev Mol Cell Biol. 2002; 3:919–931. [PubMed: 12461558]

Yarar D, Surka MC, Leonard MC, Schmid SL. SNX9 activities are regulated by multiple phosphoinositides through both PX and BAR domains. Traffic. 2008; 9:133–146. [PubMed: 17988218]

Yarar D, Waterman-Storer CM, Schmid SL. SNX9 couples actin assembly to phosphoinositide signals and is required for membrane remodeling during endocytosis. Dev Cell. 2007; 13:43–56. [PubMed: 17609109]

NIH-PA Author Manuscript
NIH-PA Author Manuscript
NIH-PA Author Manuscript

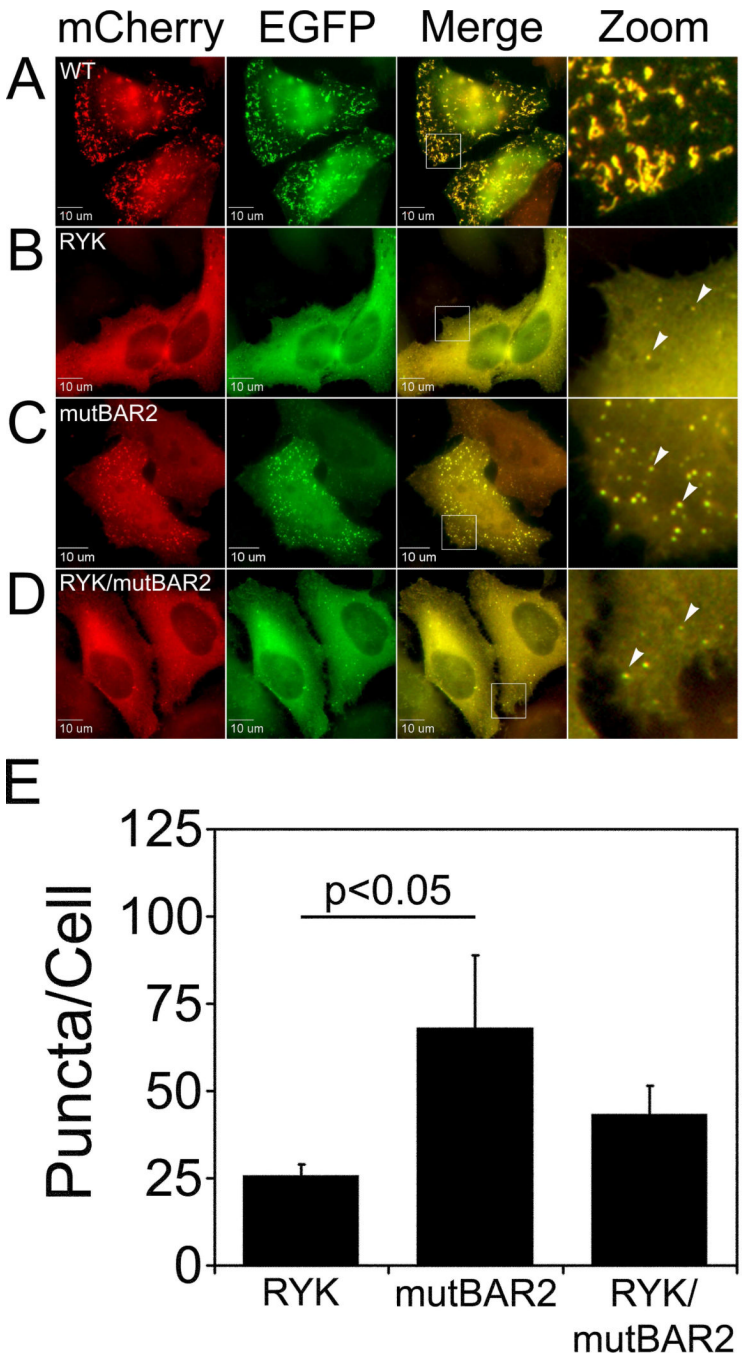

Figure 1. Point mutations in either the PX or BAR domain of SNX9 attenuate EspF-induced membrane tubulation

HeLa cells were transiently transfected with pEGFP-EspF and pmCherry-SNX9 and assessed for the formation of membrane tubules by epifluorescence microscopy. Transfection of WT mCherry-SNX9 exhibited extensive membrane tubulation (**A**). In contrast, expression of SNX9 containing point mutations in either the PX (**B**), BAR (**C**), or both domains (**D**) did not induce membrane tubule formation. In these cells, mCherry-SNX9 and EGFP-EspF co-localized to punctate areas (arrowheads). (**E**) Quantification of punctate areas per cell from images represented in panels B, C and D. Images are representative of three independent experiments.

NIH-PA Author Manuscript

NIH-PA Author Manuscript

NIH-PA Author Manuscript

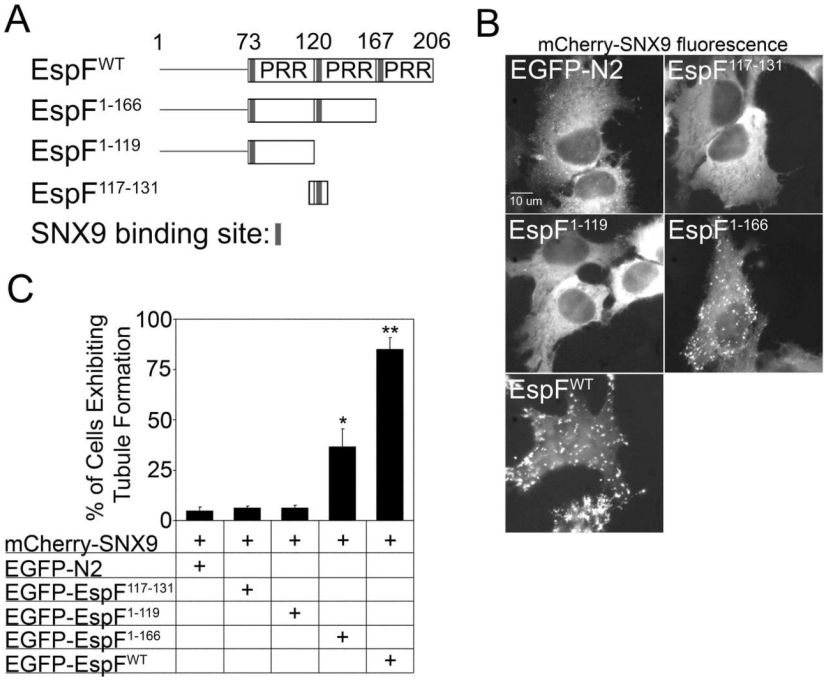

Figure 2. SNX9 binding by EspF is not sufficient to induce membrane tubulation

A. Schematic representation of EspF constructs. Wild-type EspF (EspF^{WT}) contains three carboxy-terminal proline-rich repeats (PRR), each of which contains one 7aa SNX9 binding site (gray rectangle). **B.** HeLa cells cotransfected with pmCherry-SNX9 and either pEGFP-N2, pEGFP-EspF$^{117-131}$, or pEGFP-EspF$^{1-119}$ displayed normal cellular distribution of mCherry-SNX9. In cells expressing EGFP-EspF$^{1-166}$ or EGFP-EspF^{WT}, mCherry-SNX9 was localized to tubular vesicles. **C.** Quantitation of B. 100 HeLa cells co-expressing mCherry-SNX9 and EGFP constructs were evaluated for the presence or absence of tubular structures over three independent experiments. Expression of EGFPEspF$^{117-131}$ or EGFP-EspF$^{1-119}$ did not increase the number of mCherry-SNX9-expressing cells with tubules as compared to expression of the pEGFP-N2 vector. Expression of EGFP-EspF$^{1-166}$ induced a significant increase ($p<0.05$) in tubule formation in comparison to EGFP-N2, EGFP-EspF$^{117-131}$ and EGFP-EspF$^{1-119}$. The percent of cells exhibiting tubules was significantly higher ($p<0.05$) in cells expressing EGFP-EspF^{WT} than in all other conditions.

NIH-PA Author Manuscript
NIH-PA Author Manuscript
NIH-PA Author Manuscript

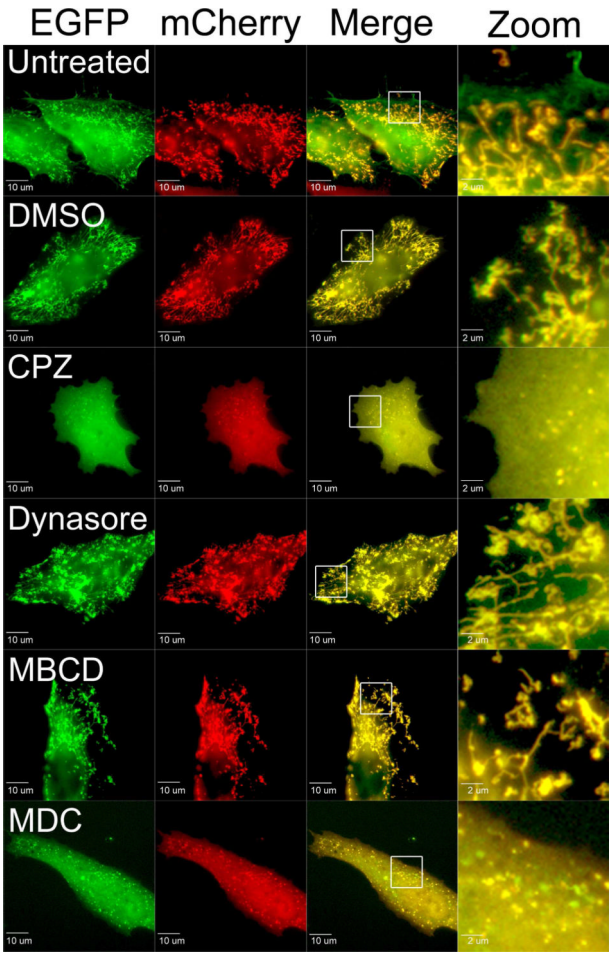

Figure 3. Chlorpromazine and monodansyl cadaverine block EspF/SNX9-induced membrane tubulation

HeLa cells co-transfected with EGFP-EspF and mCherry-SNX9 were incubated with DMEM (Untreated), or DMEM with 0.1% DMSO, 60μM chlorpromazine (CPZ), 80μM dynasore, 10mM methyl-beta-cyclodextrin (MBCD), or 400μM monodansyl cadaverine (MDC). Inhibitor treatment did not affect expression levels of either transgene. Both EGFP-EspF and mCherry-SNX9 localized to tubules in all conditions except treatment with CPZ and MDC, in which case both proteins exhibited a punctate staining pattern. Images are representative of three independent experiments.

NIH-PA Author Manuscript

NIH-PA Author Manuscript

NIH-PA Author Manuscript

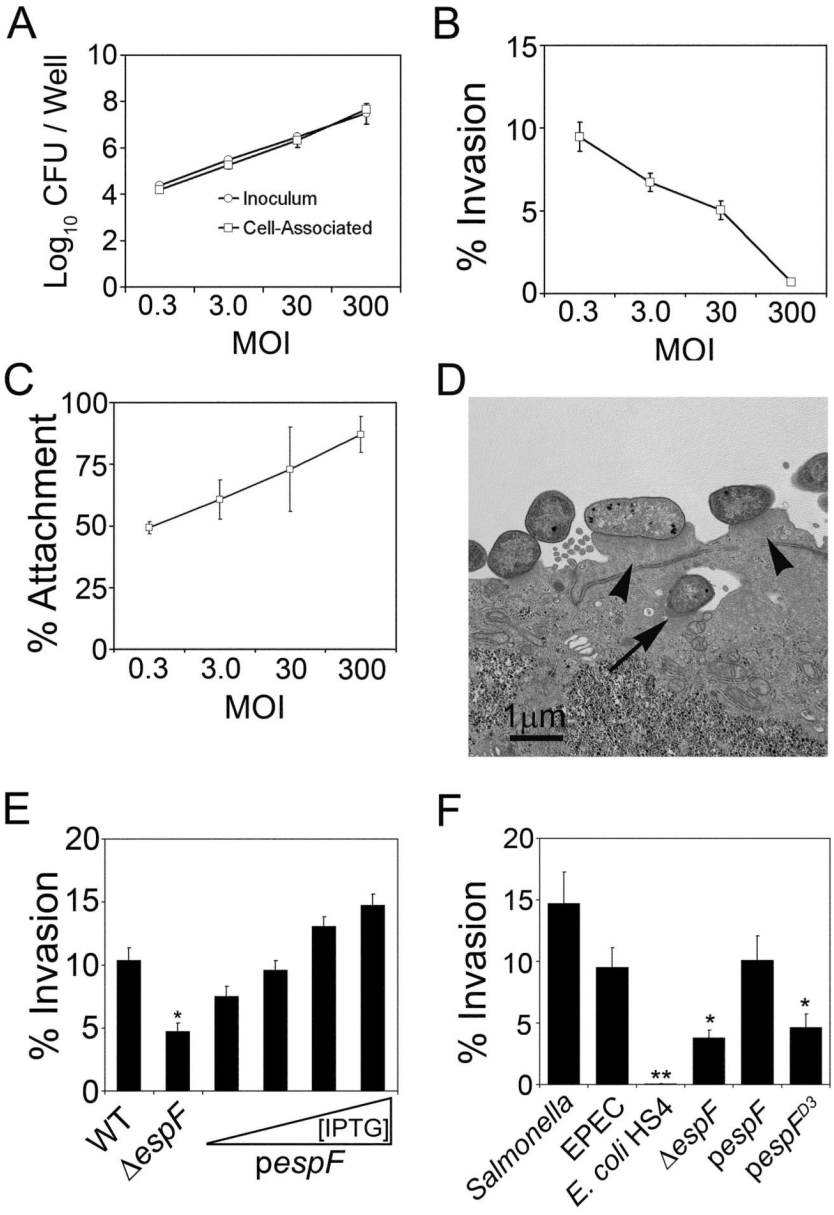

Figure 4. EPEC invasion of Caco-2 intestinal epithelial cells is dependent on EspF/SNX9 interaction

A. Inoculum (○) and total cell-associated bacteria (□) represented as CFU per well of 24-well plates from three independent gentamicin protection assays (GPAs) performed on Caco-2 cells infected with EPEC at MOIs of 0.3, 3, 30 and 300. **B.** Intracellular CFU per well from the GPAs in A were divided by total cell associated CFU per well and multiplied by 100 to give % invasion. **C.** Total cell-associated CFU per well were divided by the inoculum and multiplied by 100 to give % attachment. **D.** Transmission electron microscopic image of Caco-2 cells grown on Transwell permeable supports for 17 days and infected with WT EPEC. The arrow indicates an intracellular bacterium, pedestals are indicated by arrowheads. **E.** GPAs performed on Caco-2 cells infected with wild-type EPEC (WT), an *espF* deletion mutant (Δ*espF*) or Δ*espF* complemented with the *espF* gene on an IPTG-inducible plasmid (p*espF*). Ramp represents treatment of p*espF* with IPTG concentrations of 0, 1, 10, or 100 μM. **F.** Invasion of Caco-2 cells by *Salmonella* (ATCC

14028), WT EPEC, the commensal *E. coli* isolate HS4, Δ*espF*, p*espF*, or p*espF*^{D3}, an espF point mutant expressing SNX9 binding deficient EspF. All results are representative of three independent experiments. *: $p<0.05$. **: $p<0.05$ as compared to*.

NIH-PA Author Manuscript
NIH-PA Author Manuscript
NIH-PA Author Manuscript

NIH-PA Author Manuscript

NIH-PA Author Manuscript

NIH-PA Author Manuscript

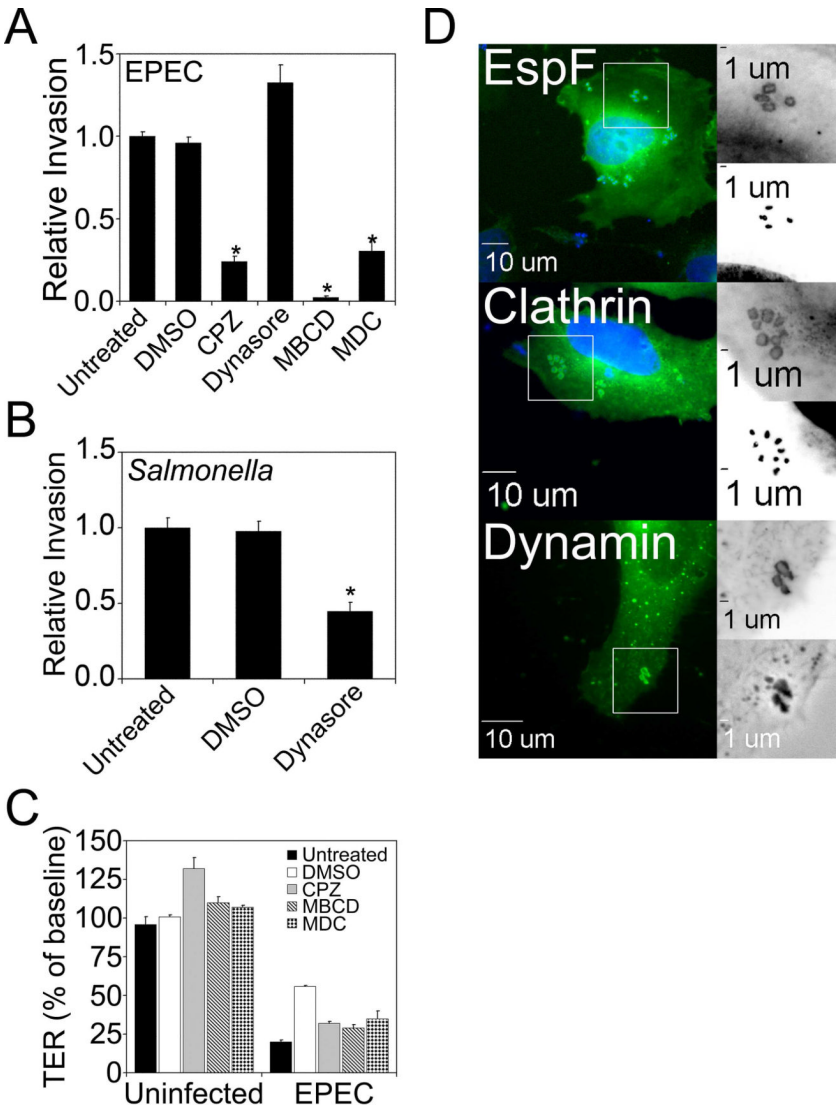

Figure 5. Inhibitors of CME and lipid rafts block EPEC invasion but not EPEC-induced TER loss

A. Gentamicin protection assays in Caco-2 cells infected with wild-type EPEC suspended in serum-free DMEM (Untreated) or serum-free DMEM with 0.1% DMSO, 60μM chlorpromazine (CPZ), 80μM dynasore, 10mM methyl-beta-cyclodextrin (MBCD), or 400μM monodansyl cadaverine (MDC). Invasion was significantly inhibited in cells treated with CPZ, MBCD, or MDC. *: $p<0.05$. Bacterial attachment was not affected by inhibitor treatment (data not shown). Relative invasion was calculated as described in *Methods* and WT normalized to 1.0. **B.** GPAs performed as in **A** but with *Salmonella* in the presence of media alone (Untreated), 0.1% DMSO or 80μM dynasore. Dynasore treatment significantly reduced the rate of *Salmonella* invasion. *: $p<0.05$. **C.** Caco-2 cells were grown on permeable supports for 14 days and transepithelial electrical resistance (TER) was measured after treatment with serum-free DMEM (Uninfected) or serum-free DMEM with wild-type EPEC (EPEC) for 6 hours. TER was significantly reduced by EPEC infection in the presence of media alone (Untreated) or media with 0.1% DMSO, 60μM chlorpromazine (CPZ), 10mM methyl-beta-cyclodextrin (MBCD), or 400μM monodansyl cadaverine (MDC). Inhibitor treatment alone did not reduce TER. **D.** HeLa cells transiently transfected

with either EGFP-EspF (EspF), YFP-clathrin light chain (Clathrin) or EGFP-dynamin II (Dynamin) were infected for 2.5 hours with wild-type EPEC and processed for epifluorescent microscopy. All three fluorescent fusion proteins were found to accumulate around attached bacteria, shown by DAPI staining (EspF, Clathrin) or by phase contrast (Dynamin).

NIH-PA Author Manuscript
NIH-PA Author Manuscript
NIH-PA Author Manuscript

NIH-PA Author Manuscript

NIH-PA Author Manuscript

NIH-PA Author Manuscript

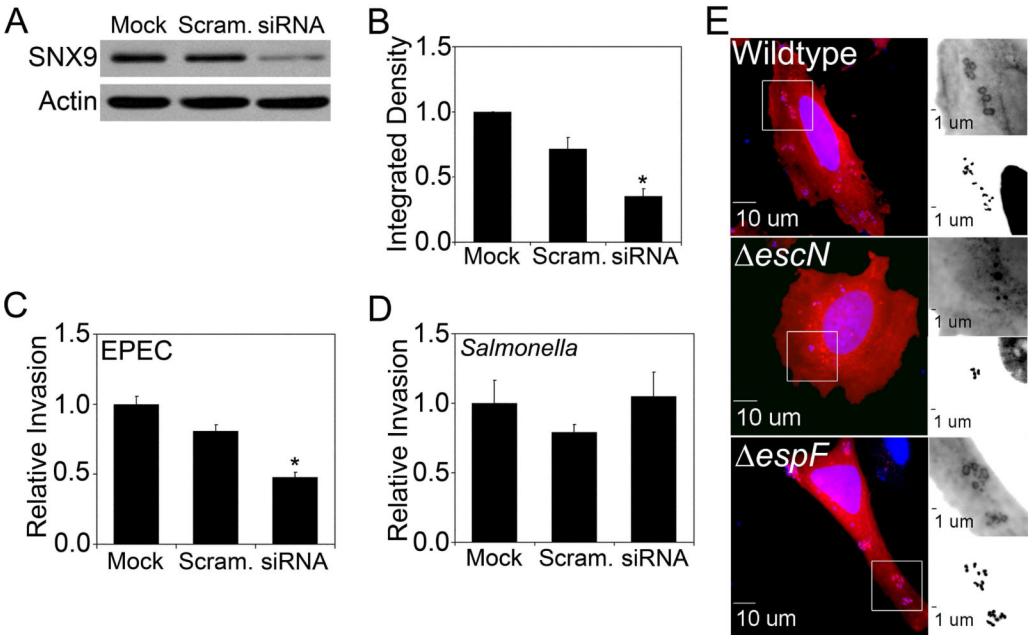

Figure 6. Depletion of SNX9 by siRNA significantly reduced invasion of Caco-2 cells by EPEC, but not *Salmonella*

A. Western blot of Caco-2 cells three days after electroporation without oligonucleotide (Mock), with a scrambled RNA oligonucleotide (Scram.), or with SNX9-specific siRNA (siRNA). Image is representative of 6 independent experiments. SNX9 protein levels were assessed in parallel with EPEC and *Salmonella* invasion assays. **B.** Integrated density analysis of 6 Western blots represented in A. Values are indicative of SNX9 band density relative to actin band density. *: $p<0.05$. **C.** Gentamicin protection assays of Caco-2 cells described in A and infected with WT EPEC at an MOI of 0.3. *: $p<0.05$. **D.** Gentamicin protection assays of Caco-2 cells described in A and infected with *Salmonella* at an MOI of 0.3. *: $p<0.05$.

NIH-PA Author Manuscript
NIH-PA Author Manuscript
NIH-PA Author Manuscript

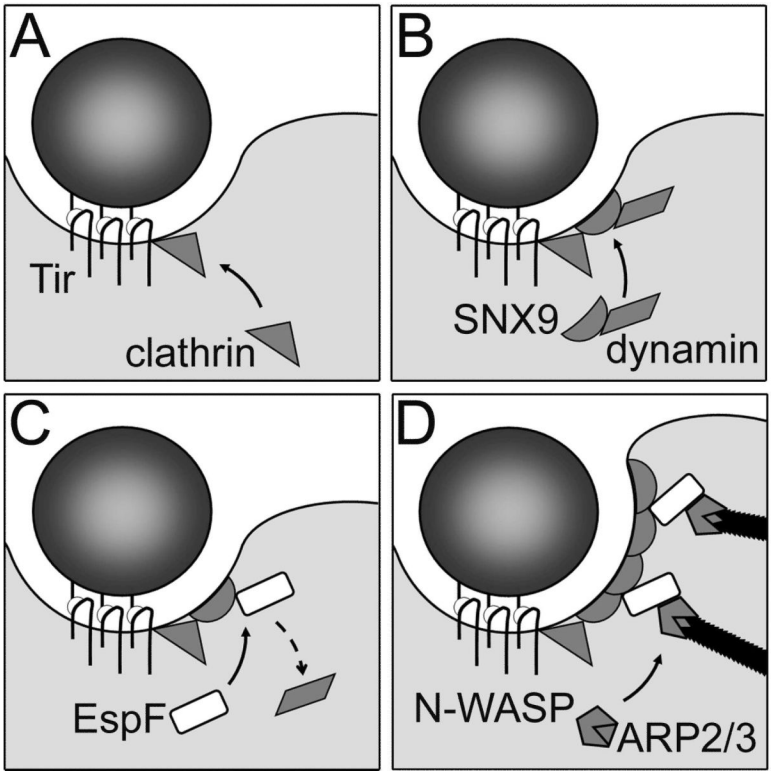

Figure 7. Model of SNX9 recruitment and activation during EPEC invasion

A. After injection into the cytosol of epithelial cells, the translocated intimin receptor (Tir) is inserted into the plasma membrane, permitting it to interact with the EPEC surface protein intimin. Tir is known to recruit clathrin, leading to its accumulation at sites of EPEC attachment. **B.** The combination of EPEC-induced membrane curvature, clathrin assembly and PIP accumulation, all of which are documented to occur upon EPEC attachment, may provide a plasma membrane environment favorable to SNX9 recruitment. Under normal conditions, SNX9 recruits its binding partner dynamin to these membrane domains. **C.** EspF interacts with the SH3 domain of SNX9 subsequent to its membrane recruitment. EspF then outcompetes with dynamin for interaction with the SNX9 SH3 domain. **D.** The presence of multiple SNX9 binding domains permits EspF to bind up to three SNX9 molecules, inducing SNX9 oligomerization and increased membrane deforming activity. This, coupled with N-WASP-dependent actin polymerization by EspF, enhances EPEC invasion.